Final Report

SSME LOX POST FLOW ANALYSES/FLUID STRUCTURE INTERACTION

Contract NAS8-35505

20 September 1988

(NASA-CR-183538) SSME LOX POST FLOW ANALYSES/FLUID STRUCTURE INTERACTION Final Report (Lockheed Missiles and Space Co.) 25 p CSCL 20D

N89-13758

Unclas G3/34 0183260

Prepared for

NATIONAL AERONAUTICS AND SPACE ADMINISTRATION
MARSHALL SPACE FLIGHT CENTER, AL 35812

Prepared by

Lockheed
Missiles & Space Company, Inc.
Huntsville Engineering Center
4800 Bradford Blvd., Huntsville, AL 35807

FOREWORD

Lockheed Missiles & Space Company, Inc., Huntsville Engineering Center, submits this final report to NASA-Marshall Space Flight Center as fulfillment of Contract NAS8-35505. The NASA technical monitor for this contract was Homer B. Wilson, Jr., EB31.

CONTENTS

Section		Page
	FOREWORD	ii
1	INTRODUCTION	1
2	TECHNICAL APPROACH	3
	2.1 General	3
	2.2 Flowfield Computations	4
3	FLOWFIELD RESULTS	9
4	CONCLUSIONS AND RECOMMENDATIONS	21
5	REFERENCES	22

LIST OF FIGURES

Figure		Page
1	SSME Power Component Arrangement	2
2	SSME LOX Post Array	2
3	C Grid Used in Trial Steady State Calculations	5
4	Mesh System for Unsteady Computations	6
5	Mesh System Showing Multiple Posts in Streamwise Direction	7
6	Velocity Vectors for Trial Steady State Calculation	10
7	Pressure Contours for Trial Steady State Calculation	10
8	Velocity Vectors Showing Development of Unsteady Behavior	11
9	Velocity Vectors in near Wake at t = 103.75	12
10	Velocity Vectors in near Wake at t = 112.50	13
11	Velocity Vectors in far Wake at t = 103.75	14
12	Velocity Vectors in far Wake at t = 112.50	15
13	Velocity Magnitude Contours Approximately One-Half Cycle Apart	17
14	Velocity Magnitude Contours at Time Step of t = 2.5	18
15	Pressure Contours at t = 103.75	19
16	Pressure Contours at t = 112.50	19
17	Pressure Distribution on Cylinder at t = 103.75	20

1. INTRODUCTION AND SUMMARY

Test firings of the Space Shuttle Main Engine (SSME) over the course of its development have resulted in several catastrophic failures. Some of these failures were due to breakage of the LOX posts that feed liquid oxygen into the main injector head of the engine. The overall arrangement of the primary components of the SSME is shown in Fig. 1. The LOX post array in the main injector is shown in Fig. 2. Hot turbine gases flow from the high pressure hydrogen and oxygen turbopumps through the hot gas manifold transfer ducts and into the main injector. The LOX posts are subjected to severe thermal and gasdynamic loads due to impingement of the hot gases onto the posts. The unsteady shedding of vortices from the posts produce fluctuating pressure loads, and the deforming structural response of the posts to these loads affects the gas flow field by producing a moving flowfield boundary. Thus, the flow field and structural response are coupled dynamically in an unsteady system.

The objective of this study was to perform a computational fluid flow analysis of a simplified SSME LOX post array using an existing viscous Navier-Stokes flow solver. A two-dimensional analysis was to be made. In addition, a finite element theory for treating the fluid/structure interaction between the posts and the hot gas environment was to be developed.

The methodology used in computing the flow field through the LOX post array is described in Section 2. Results are presented in Section 3, and concluding remarks in Section 4.

ORIGINAL PAGE IS
OF POOR QUALITY

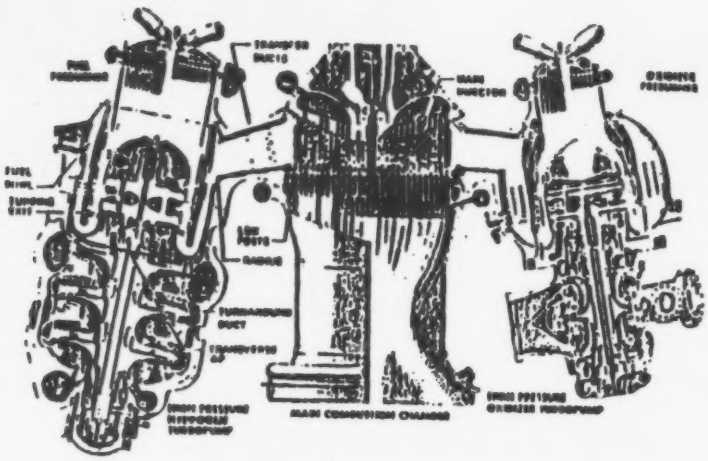

Fig. 1 SSME Power Component Arrangement

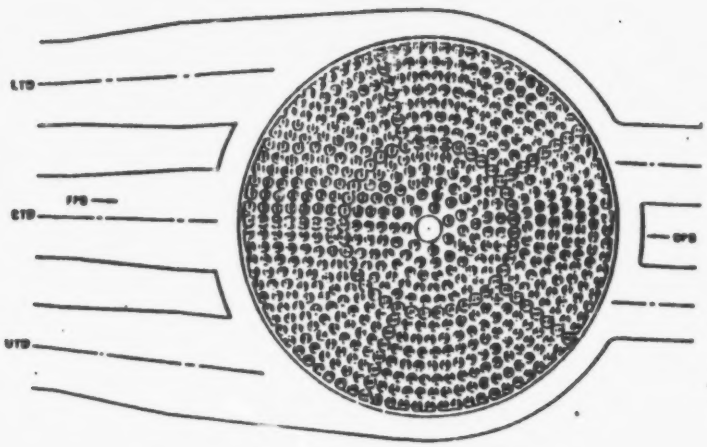

Fig. 2 SSME LOX Post Array

2. TECHNICAL APPROACH

2.1 GENERAL

The calculations were performed using the incompressible, implicit INS3D flow solver developed at NASA-Ames (Ref. 1). The INS3D code solves the three-dimensional incompressible Navier-Stokes equations in primitive variables. An implicit finite difference operator is used in a general curvilinear coordinate system. The solution procedure uses the standard approximate factorizaion scheme. The pressure field solution is based on the concept of adding a time-like pressure term into the continuity equation via an artificial compressibility factor. This approach was first introduced by Chorin (Ref. 1) and later adopted by Steger and Kutler (Ref. 2) using an implicit approximate factorization scheme by Beam and Warming (Ref. 3). INS3D evolved from these earlier developments (Ref. 4).

Values of the artificial compressibility factor are bounded in order not to influence the steady state mass conservation. In the INS3D methodology, mass conservation is of crucial importance if a stable solution is to result. Since the continuity equation is modified to obtain a hyperbolic-type equation, pressure waves of finite speed will be introduced. The speed of propagation of these pressure waves depends on the magnitude of the compressibility parameter. When the pressure waves travel through a given location, a pressure gradient is created. Near boundaries, the viscous boundary layer must respond to this pressure fluctuation. To accelerate convergence and avoid slow fluctuations, it is desirable that the time required for pressure waves to propagate through the region of interest be much less than the time needed for the boundary layer to fully adjust itself. This condition provides for a lower bound on the artificial compressibility factor. The upper bound on this factor comes not from the physics but from the effects of the

approximate factorization of the governing equations. When the finite difference form of the equation is factored, higher order cross-differencing terms are added to the left-hand side of the equation. These added terms must be made smaller than the original terms everywhere in the computational domain. This condition results in an upper bound on the compressibility factor.

2.2 FLOWFIELD COMPUTATIONS

As a trial case, steady state numerical computations were performed around a single post, with periodic boundary conditions used to simulate a row of posts. Figure 3 shows the C grid used in these calculations. The inlet of the grid is located two post diameters upstream of the post, with the exit plane located four diameters downstream. The periodic side boundaries are located one and one-half post diameters away from the post center, thus representing a row of posts separated by two post diameters.

Following the completion of the steady state test case, unsteady computations were performed for the regular grid shown in Fig. 4. As in the steady state case, periodic boundary conditions are applied at the lateral boundaries of the computational domain to simulate a row of posts. In contrast to the C grid used earlier, where the boundary was placed half-way between the two posts, the boundary for the grid shown in Fig. 4 is located at the post centerline. This configuration facilitates the addition of multiple posts, as shown in Fig. 5.

In order to investigate unsteady motion around the LOX posts, it was necessary to introduce a perturbation into the flow field. This was accomplished by rotating the post at a small angular velocity for 50 iterations, and then holding the post fixed for the remainder of the calculation. The nondimensional time step used in the calculations was 0.05, with an angular velocity of 0.01 radians/unit time. Even though INS3D is designed primarily for obtaining steady state solutions, it is capable of showing the qualitative nature of unsteady problems (Ref. 2).

ORIGINAL PAGE IS
OF POOR QUALITY

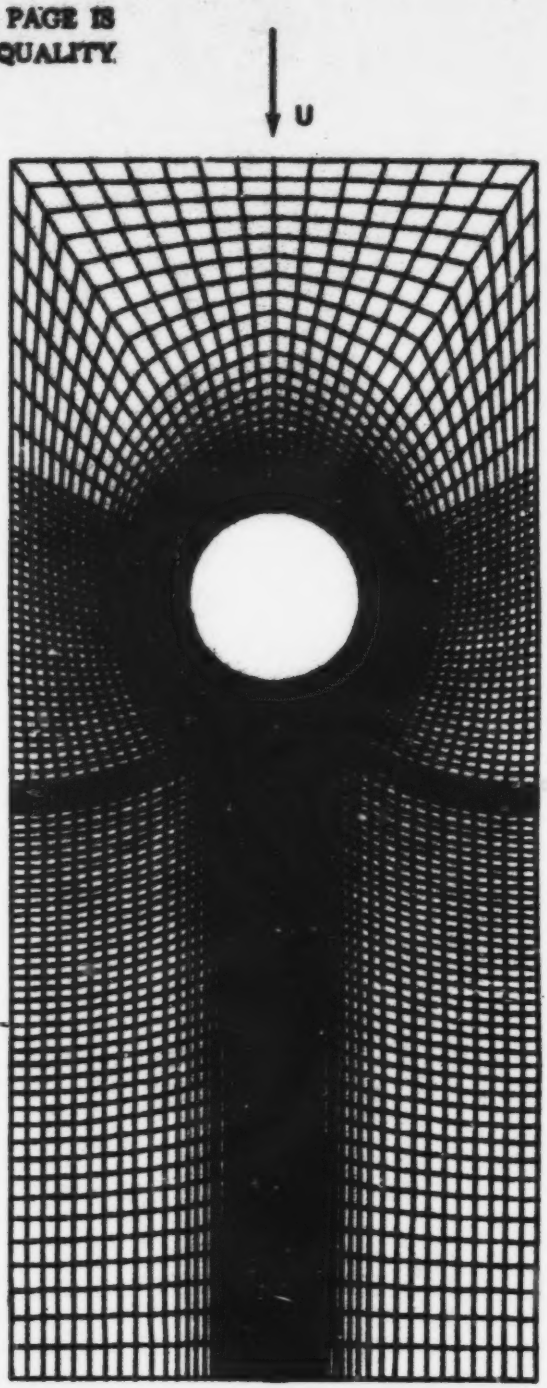

Fig. 3 C Grid Used in Trial Steady State Calculations

ORIGINAL PAGE IS
OF POOR QUALITY

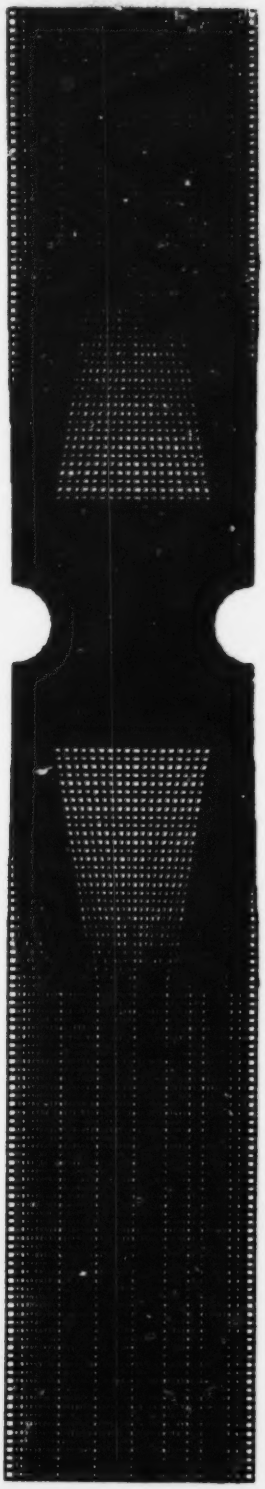

Fig. 4 Mesh System for Unsteady Computations

ORIGINAL PAGE IS
OF POOR QUALITY

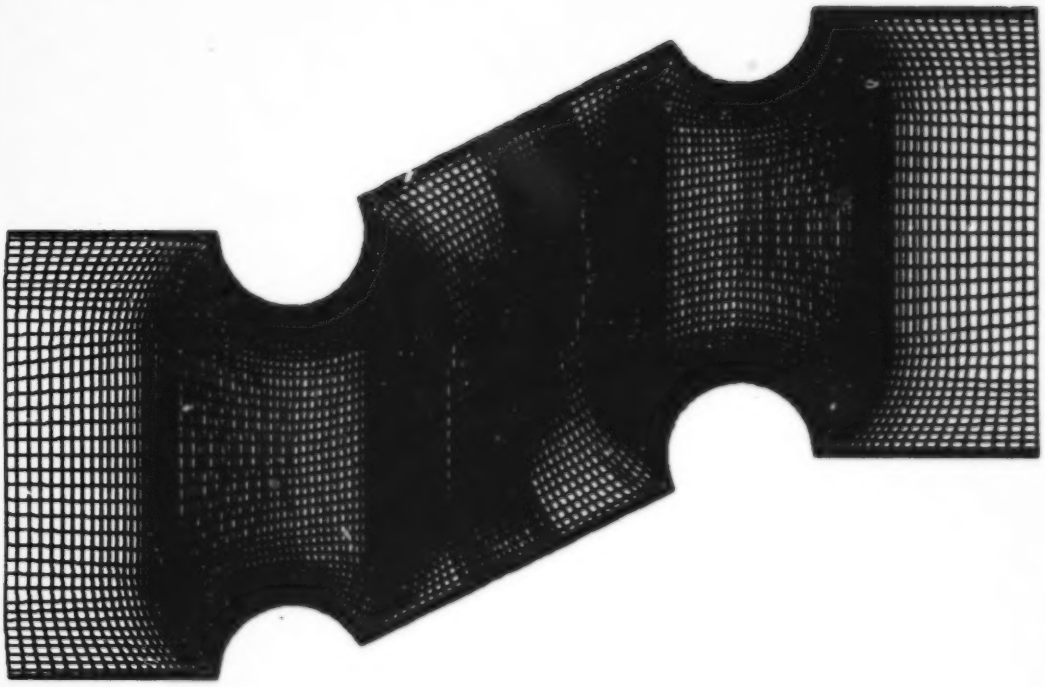

Fig. 5 Mesh System Showing Multiple Posts in Streamwise Direction

Explicit boundary conditions were used for both the steady and unsteady calculations. At the inlet plane the total pressure was held constant, and

$$\frac{\partial^2 p}{\partial x^2} = 0.0$$

where p is the static pressure.

At the exit the values of velocity and pressure were determined in the manner prescribed by Chang et al. (Ref. 4). In this technique a second-order upwind extrapolation is first used to update the velocities. Next, these updated velocities are mass-weighted to conserve the inlet mass flux. A new pressure corresponding to these mass-weighted velocities is then obtained to ensure conservation of momentum flux at the outflow.

On the post surface the normal derivative of pressure is set equal to zero, i.e.,

$$\frac{\partial p}{\partial n} = 0.0 \ .$$

For the steady state trial case the velocity is set equal to zero. For the unsteady case the velocity is determined in the manner described above.

3. FLOWFIELD RESULTS

Two-dimensional steady state laminar results were obtained for the flow around a single post, with periodic boundary conditions to simulate a row of posts. The Reynolds number, based on the post diameter, was 100. Figure 6 shows the velocity vectors in the region around the post. Two symmetrical recirculation regions are observed behind the post. The length of the wake is approximately two post diameters. Figure 7 shows the pressure contours for this calculation. As expected, a region of high pressure is observed at the leading edge stagnation point, and a region of low pressure in the wake.

Two-dimensional unsteady calculations were performed for the grid shown in Fig. 4. As discussed in the previous section, the unsteady motion was initiated by rotating the post at a small angular velocity for fifty iterations at a nondimensional time step of 0.05, and then holding the post fixed. Figure 8 shows the evolution of the unsteady behavior at various times steps. At t = 25.0 a noticeable assymmetry is observed in the near wake region immediately behind the post.

Figures 9 and 10 show the velocity vectors in the near wake region for t = 103.75 and 112.50, respectively. During this time, corresponding to approximately one-half cycle, the vortex is seen to have moved from below the post centerline to a position above the post centerline. The region of highest velocity is observed to be in the gaps between adjacent posts. This is a consequence of mass conservation.

The velocity vectors in the far wake region for these two time levels are shown in Figs. 11 and 12. The flowfield pattern has a periodic nature, with the flow in Fig. 11 being 180 degrees out of phase from that of Fig. 12.

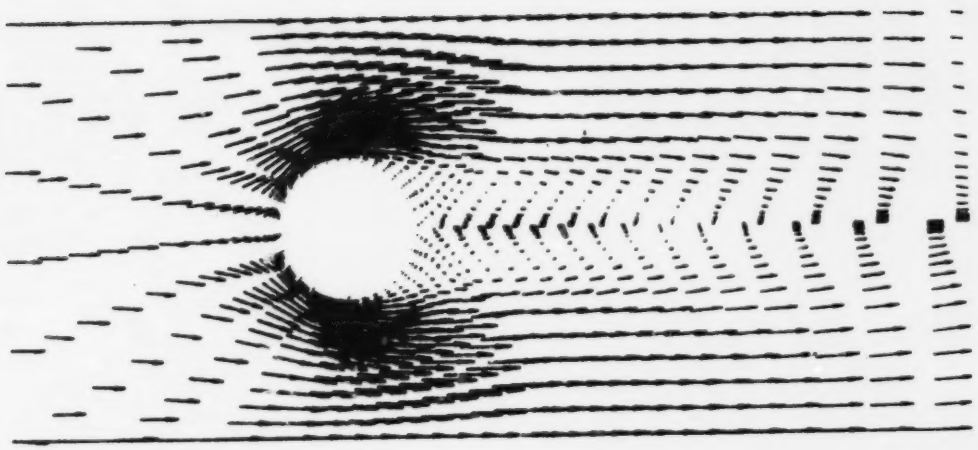

Fig. 6 Velocity Vectors for Trial Steady State Calculation

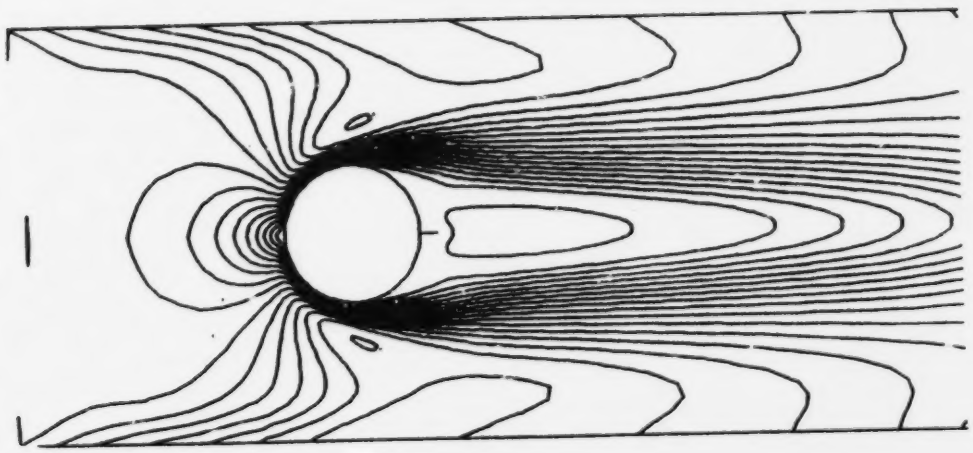

Fig. 7 Pressure Contours for Trial Steady State Calculation

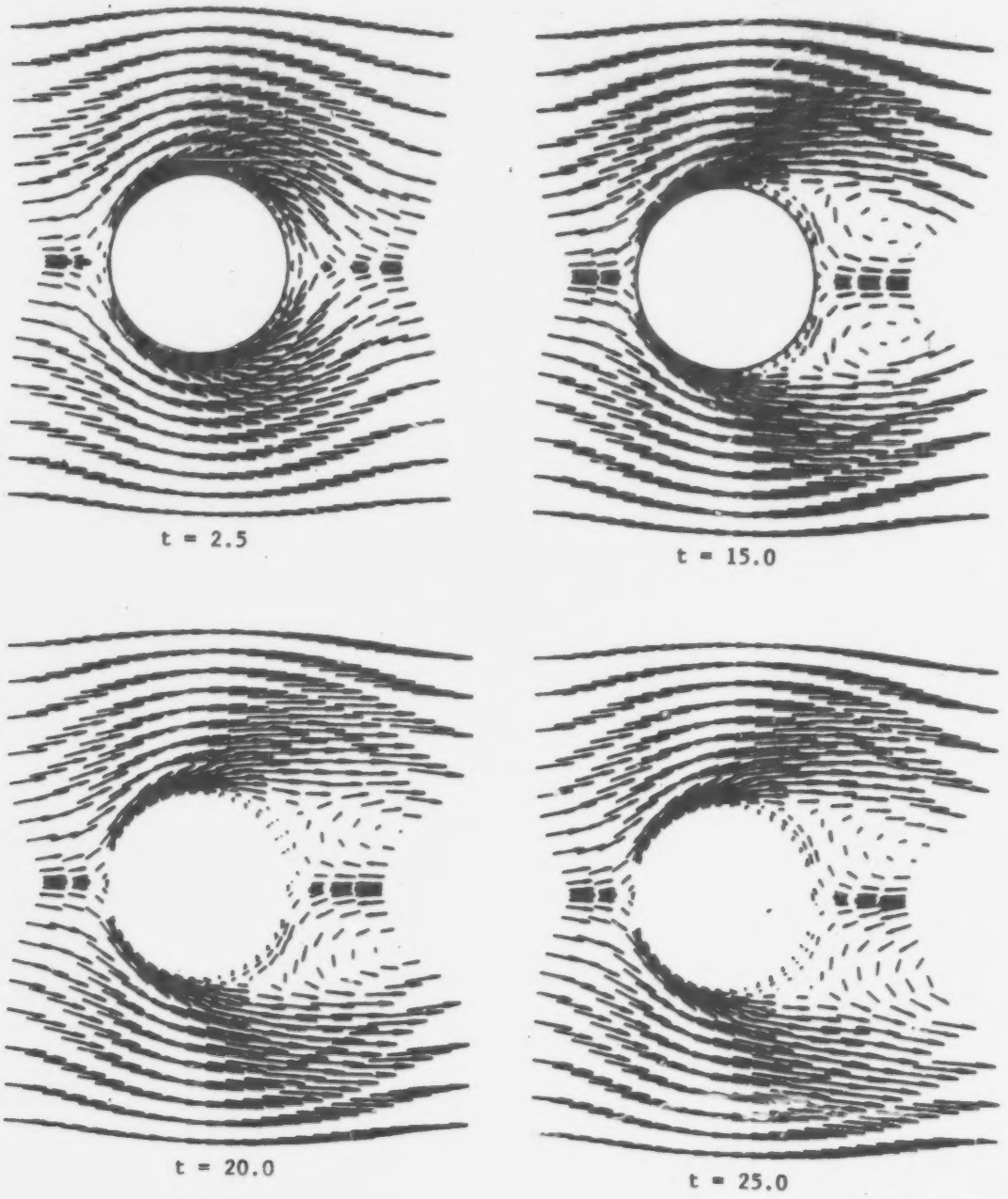

Fig. 8 Velocity Vectors Showing Development of Unsteady Behavior

ORIGINAL PAGE IS
OF POOR QUALITY

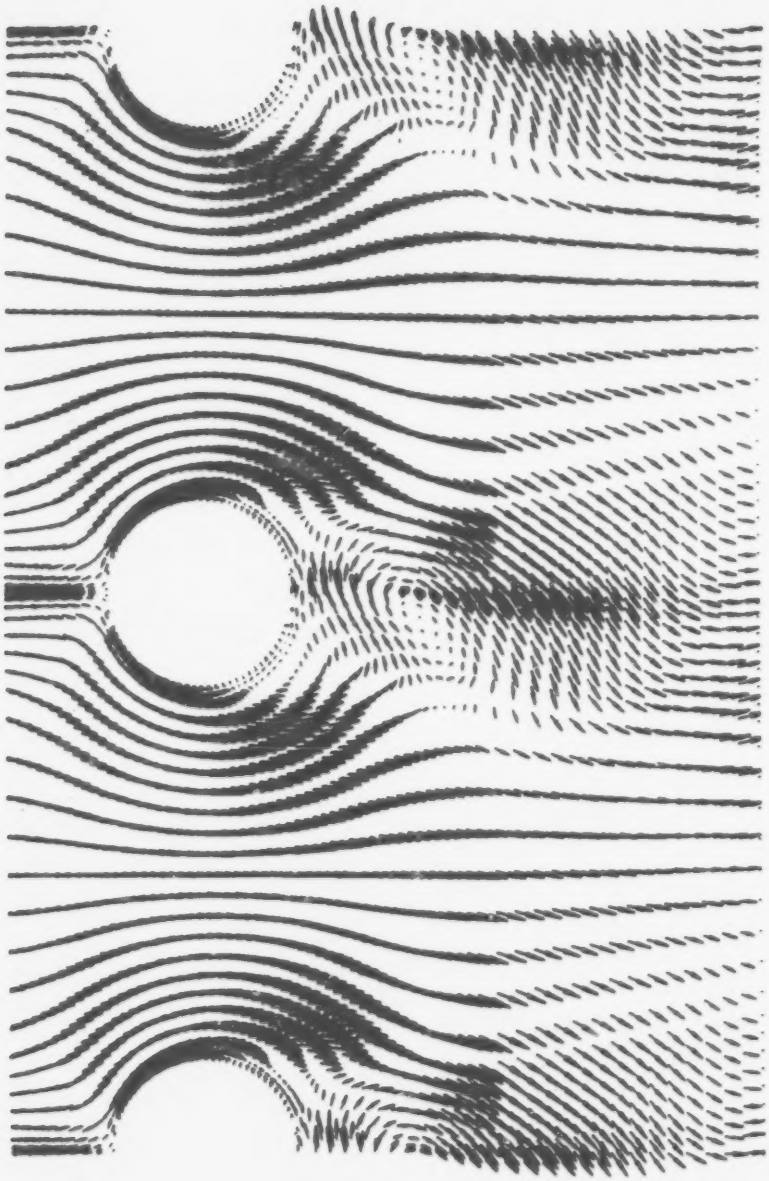

Fig. 9 Velocity Vectors in near Wake at t = 103.75

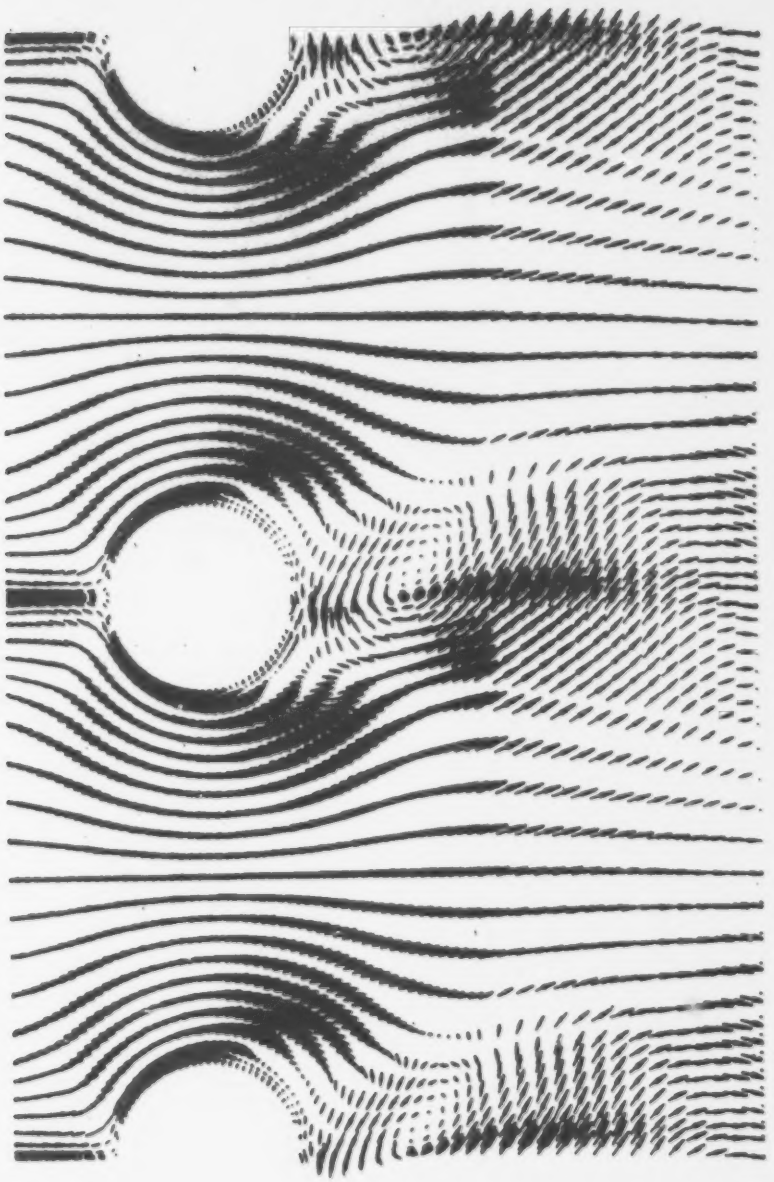

Fig. 10 Velocity Vectors in near Wake at t = 112.50

ORIGINAL PAGE IS
OF POOR QUALITY

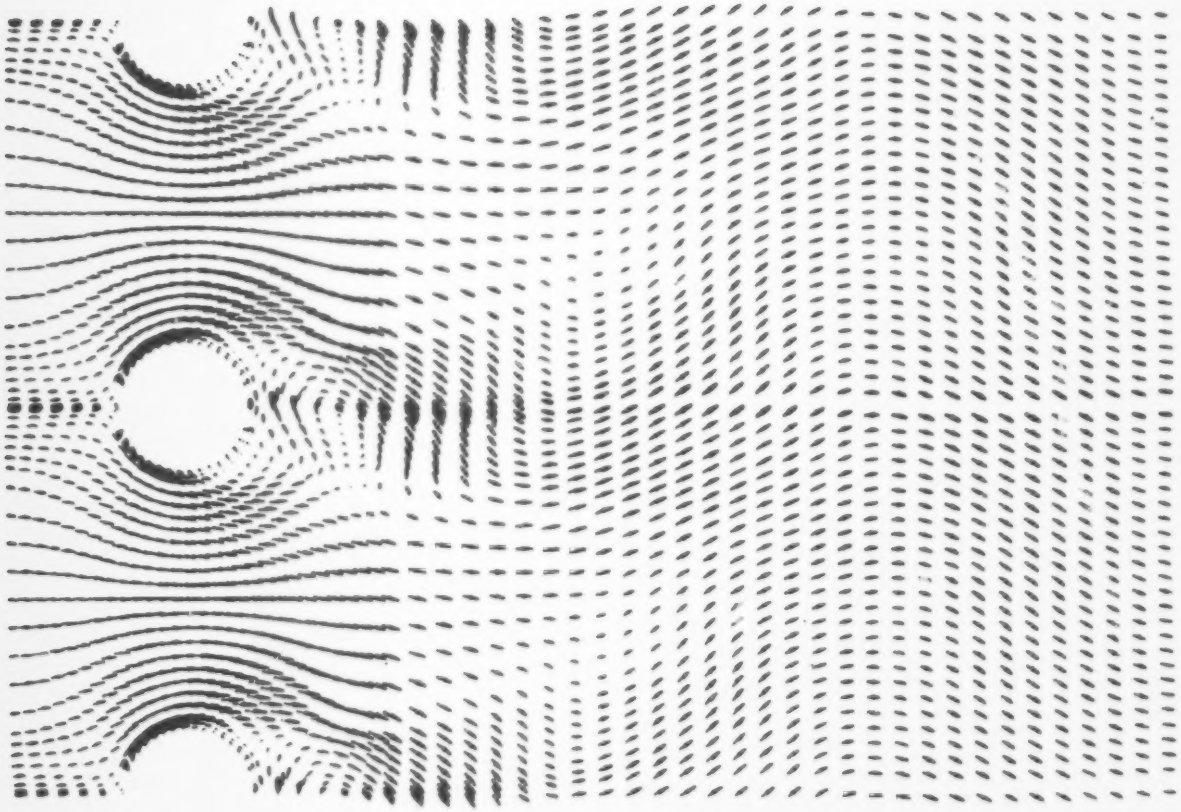

Fig. 11 Velocity Vectors in far Wake at t = 103.75

ORIGINAL PAGE IS
OF POOR QUALITY

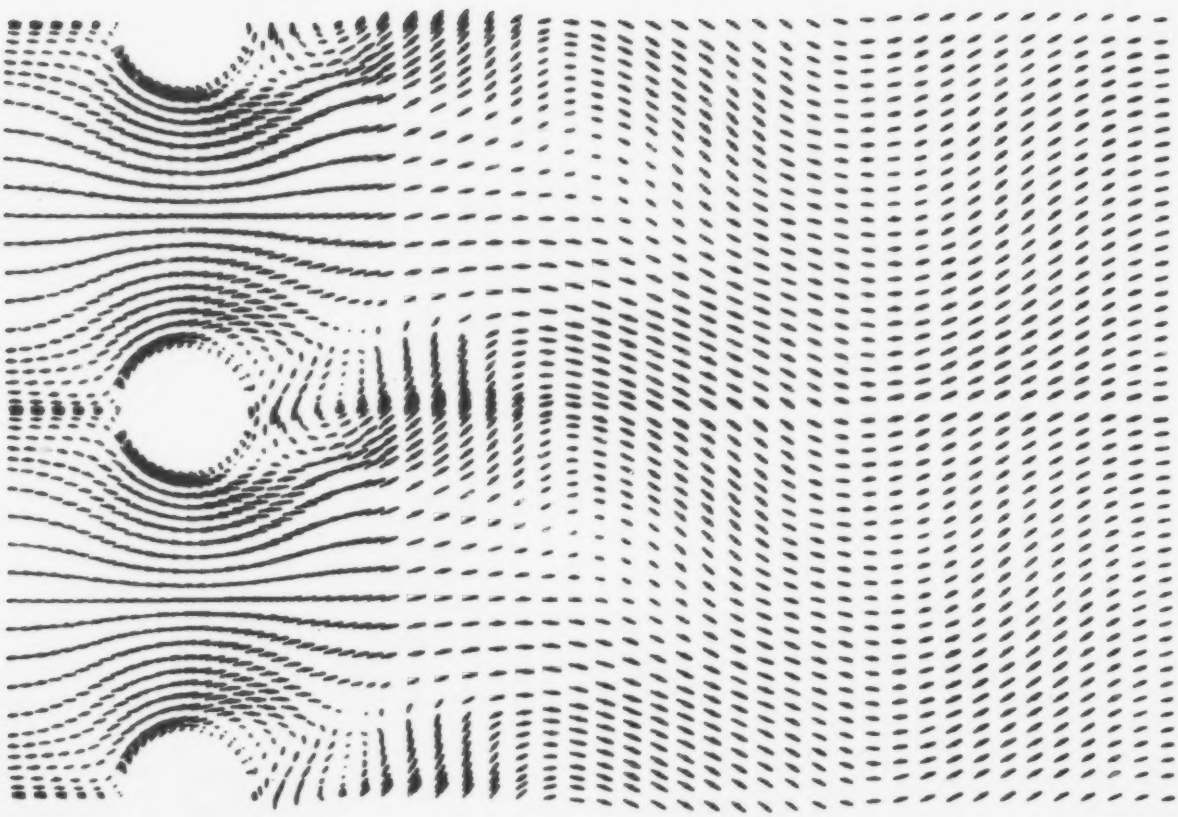

Fig. 12 Velocity Vectors in far Wake at t = 112.50

The periodic nature of the flow is further illustrated in Fig. 13, which shows the velocity magnitude contours for the two time levels, t = 103.75 and t = 112.50. Velocity magnitude contours from t = 105.0 to t = 117.5, at intervals of t = 2.5, are presented in Fig. 14. The unsteady motion of the flow, and the movement of the vortex over one-half cycle, are shown in this figure.

The pressure contours for t = 103.75 and t = 112.50 are shown in Figs. 15 and 16. A region of high pressure is observed at the leading edge stagnation point, and a region of low pressure in the wake. Figure 17 shows the pressure distribution on the post perimeter at t = 103.75. The pressure is seen to be lower on the top surface than on the bottom, thus causing a lifting force to act on the post. The direction and magnitude of this force will vary periodically with time.

t = 103.75

t = 112.50

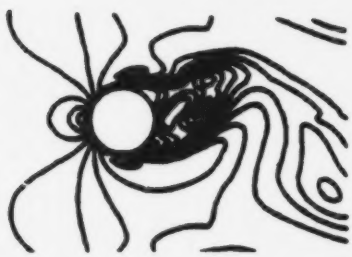

Fig. 13 Velocity Magnitude Contours Approximately One-Half Cycle Apart

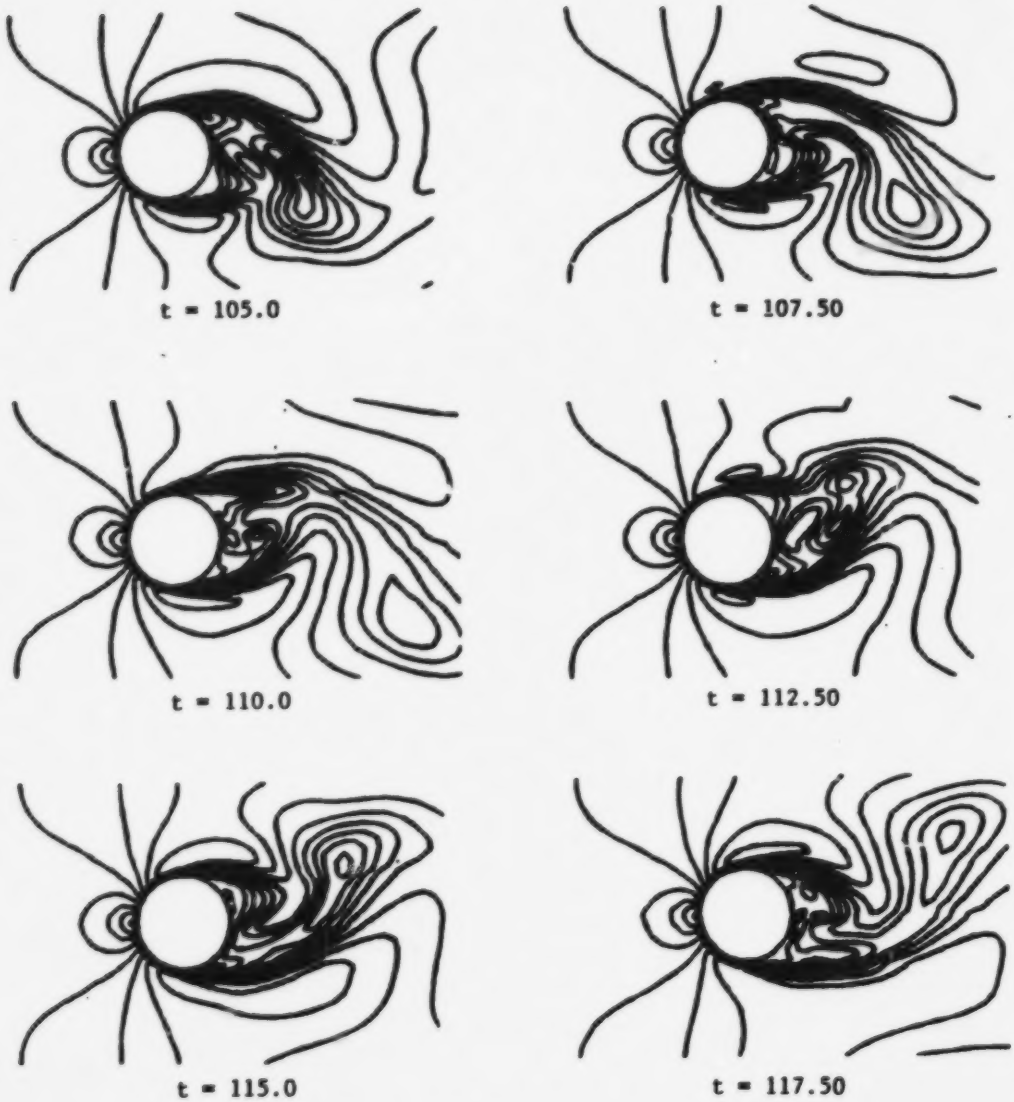

Fig. 14 Velocity Magnitude Contours at Time Step of $\Delta t = 2.5$

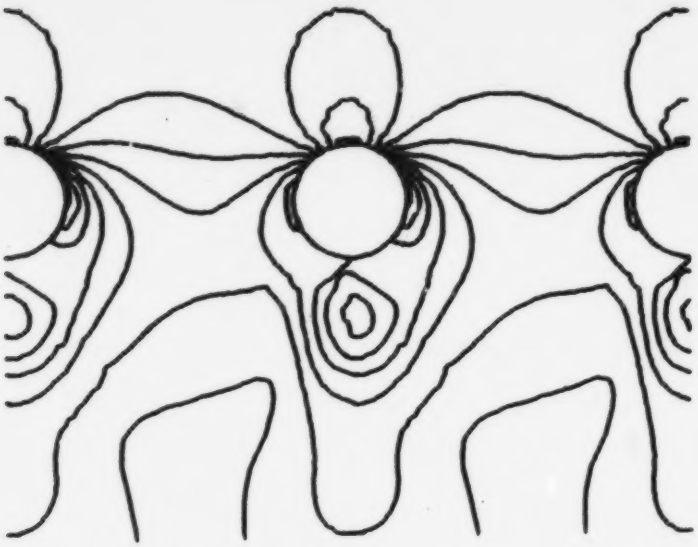

Fig. 15 Pressure Contours at t = 103.75

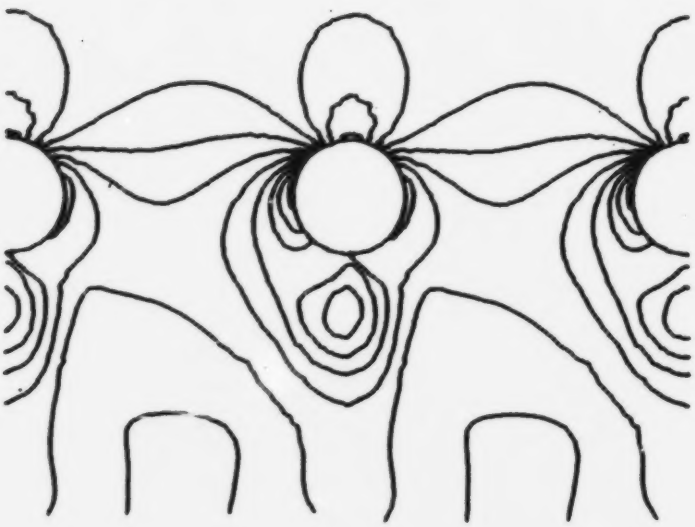

Fig. 16 Pressure Contours at t = 112.50

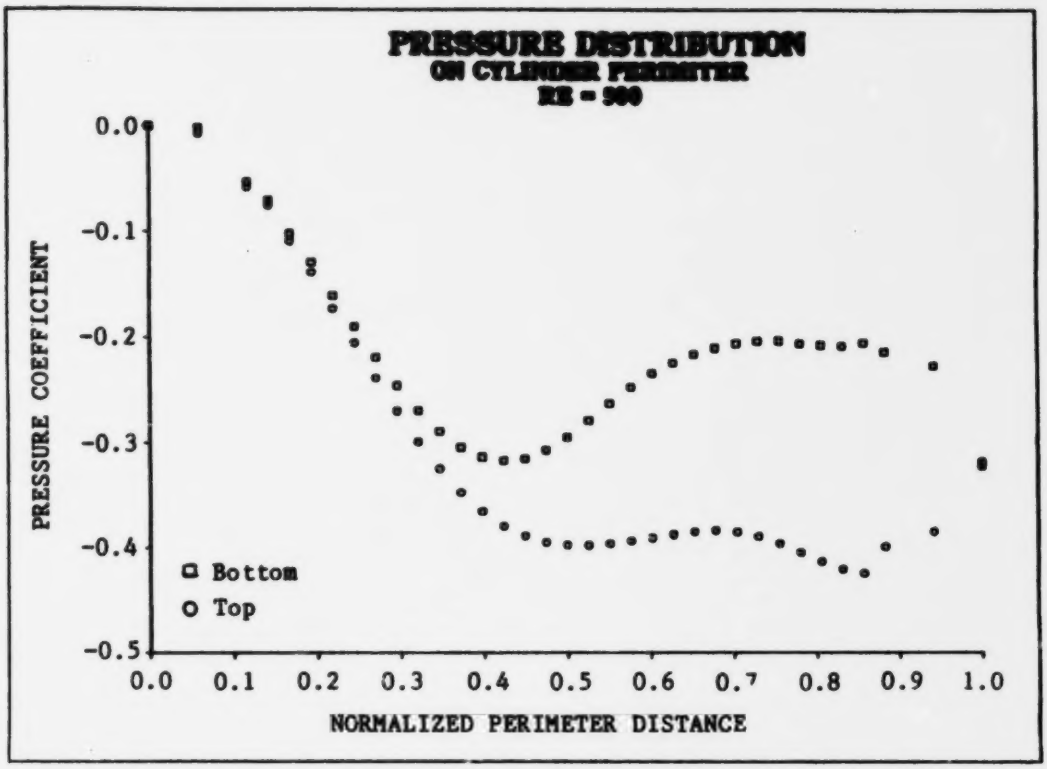

Fig. 17 Pressure Distribution on Cylinder at t = 103.75

4. CONCLUSIONS

This study has presented two-dimensional laminar results for steady and unsteady flow around arrays of posts. Only one post was considered, with periodic boundary conditions to simulate a row of posts. The unsteady motion was introduced by rotating the post surface at a small angular velocity for a fixed number of iterations, and then holding the post fixed for the remainder of the calculation. This procedure was found to introduce a periodic motion into the flow field, as observed in the patterns of velocity and pressure behind the posts. Future work would include the investigation of the effect of varying the post spacing, and of multiple posts in the streamwise direction.

5. REFERENCES

1. Chorin, A.J., "A Numerical Method for Solving Incompressible Viscous Flow Problems," J. Comp. Physics, Vol. 2, 1967, pp. 12-26.

2. Steger, J.L., and P. Kutler, "Implicit Finite-Difference Procedures for the Computation of Vortex Wakes," AIAA J., Vol 15, No. 4, 1977, pp. 581-590.

3. Beam R.M., and R.F. Warming, "An Implicit Finite-Difference Algorithm for Hyperbolic Systems in Conservation Law Form," J. Comp. Physics, Vol. 22, September 1976, pp. 87-110.

4. Kwak, D., J.L.C. Chang, S.P. Shanks, and S.R. Chakravarthy, "A Three-Dimensional Incompressible Navier-Stokes Flow Solver Using Primitive Variables," AIAA J., Vol. 24, 1986, pp. 390-396.